HHS Public Access

Author manuscript

Nat Cell Biol. Author manuscript; available in PMC 2012 February 01.

Published in final edited form as:

Nat Cell Biol. ; 13(8): 996–1003. doi:10.1038/ncb2273.

COPI acts in both vesicular and tubular transport

Jia-Shu Yang[1], **Carmen Valente**[2,3], **Roman S. Polishchuk**[2], **Gabriele Turacchio**[3], **Emilie Layre**[1], **D. Branch Moody**[1], **Christina C. Leslie**[4], **Michael H. Gelb**[5], **William J. Brown**[6], **Daniela Corda**[3], **Alberto Luini**[2,3,7], and **Victor W. Hsu**[1,7]

[1] Division of Rheumatology, Immunology and Allergy, Brigham and Women's Hospital, and Department of Medicine, Harvard Medical School, Boston, MA 02115 USA

[2] Telethon Institute of Genetics and Medicine, Via Pietro Castellino 111, 80131 Napoli, Italy

[3] Institute of Protein Biochemistry, National Research Council Via Pietro Castellino 111, 80131 Napoli, Italy

[4] Department of Pediatrics, National Jewish Medical and Research Center, and Departments of Pathology and Pharmacology, University of Colorado School of Medicine, Denver, CO 80262

[5] Department of Chemistry and Biochemistry, University of Washington, Seattle, WA 98195

[6] Department of Molecular Biology and Genetics, Cornell University, Ithaca, NY 14853

Abstract

Intracellular transport is now appreciated to occur through two general types of carriers, either vesicles [1, 2] or tubules [3, 4]. Coat proteins act as the core machinery that initiates vesicle formation [1, 2], but the counterpart that initiates tubule formation has been unclear. Here, we find that the Coat Protein I (COPI) complex initially drives the formation of Golgi buds. Subsequently, a set of opposing lipid enzymatic activities determines whether these buds become vesicles or tubules. Lysophosphatidic acid (LPA) acyltransferase type γ (LPAAT–γ) promotes COPI vesicle fission for retrograde vesicular transport. In contrast, cytosolic phospholipase A2 type α (cPLA2–α) inhibits this fission event to induce COPI tubules, which act in anterograde intra-Golgi transport and Golgi ribbon formation. These findings not only advance a molecular understanding of how COPI vesicle fission is achieved, but also shed new insight into how COPI acts in intra-Golgi transport and reveal an unexpected mechanistic relationship between vesicular and tubular transport.

[7]Address correspondence to: Victor Hsu, Tel: 617-525-1103, vhsu@rics.bwh.harvard.edu or Alberto Luini, Tel: 39-081-6132-535, luini@tigem.it.

Author contributions

J-S.Y., C.V., R.S.P., G.T., E.L., C.C.L., M.H.G., and W.J.B participated in experimental work and data analysis. V.W.H., A.L., D.B.M., and D.C. participated in project planning and data analysis. V.W.H., A.L., and J-S.Y. wrote the manuscript.

Competing financial interests

The authors declare no competing financial interests.

Keywords

vesicles; tubules; Golgi; COPI; LPAAT; cPLA2

Vesicle formation by the COPI complex has been a model system to understand how coat proteins act in vesicular transport [1, 2], largely because a vesicle reconstitution system has been established that allows detailed mechanistic studies 5. Early studies identified coatomer as coat components [6] and ARF1 as the small GTPase regulating this coat complex [7]. The GTPase-activating (GAP) that deactivates ARF1 was subsequently identified as ARFGAP1 [8], which was also found to act as an ARF effector by being a coat component [9, 10]. BARS (Brefeldin-A ADP-Ribosylated Substrate) has also been identified to act in COPI vesicle formation, having a critical role at the fission stage [11]. Membrane fission by BARS was initially attributed to a LPAAT activity that converts LPA to phosphatidic acid (PA) [12]. However, this activity was subsequently shown to be associated with, rather than intrinsic to, BARS [13]. In recent years, BARS has been found to possess an intrinsic ability to deform membrane, which requires the presence of PA as a critical lipid [14]. Moreover, the late stage of COPI vesicle fission was found to require PA generated by phospholipase D type 2 (PLD2) [14]. Notably, CI-976, a pharmacologic compound that targets LPAAT activity [15], has been shown previously to inhibit COPI vesicle formation [11]. Thus, we initially sought to delineate how both PA-generating enzymatic activities (LPAAT and PLD) could be acting in COPI vesicle formation.

When CI-976 was added to the COPI reconstitution system, we found by electron microscopy (EM) that Golgi membrane contained buds during early incubation, and then tubules of progressively longer length upon longer incubation (Fig 1a). This sequence of events was further confirmed by EM morphometry coupled to kinetic analysis (Fig 1b). Thus, rather than simply arresting COPI vesicle formation at the stage of bud formation, the inhibition of LPAAT activity by CI-976 had the additional effect of diverting COPI buds toward tubule formation.

A family of transmembrane proteins has been shown in recent years to possess LPAAT activity [16], with LPAAT-γ having been found to regulate Golgi structure and transport [17]. However, this role remains to be better defined. By confocal microscopy, we found that LPAAT-γ had a distribution at the Golgi that colocalized with coatomer (Fig S1a). To determine whether LPAAT–γ acted in COPI transport, we initially tracked the redistribution of a COPI cargo (VSVG-KDELR) from the Golgi to the ER, as previously described [11, 14, 18]. In cells treated with siRNA against LPATT-γ, we found that this redistribution was inhibited. This inhibition could be rescued by a siRNA-resistant form of the wild-type LPAAT-γ, which was abrogated by a catalytic dead mutation (Fig 1c). Revisiting the COPI reconstitution system, we found that vesicle formation was inhibited upon the addition of an anti-LPAAT–γ antibody (Fig 1d). Examining the Golgi membrane in this setting, we again observed buds followed tubules of progressive longer lengths (Fig S1b). Thus, we concluded that CI-976 likely targeted LPAAT–γ on Golgi membrane to inhibit COPI vesicle formation and promote tubule formation.

We next considered that phospholipase A2 (PLA2) activity should oppose the enzymatic activity of LPAAT, by converting PA to LPA [19]. Pharmacologic inhibitors have been developed, with MAFP (methylarachidonyl-fluorophosphonate) targeting cytosolic forms of cPLA2 (Group IV members), while BEL (bromoenol lactone) targeting preferentially a subfamily within this group (known as calcium-independent cPLA2) [19]. We found that MAFP promoted COPI vesicle formation, but BEL did not (Fig S2a). These results were further confirmed by dose-response analysis (Fig S2b). Thus, we concluded that a calcium-dependent Group IV cPLA2 was acting to inhibit COPI vesicle formation.

A member of this group, cPLA2–α, has been found to have a Golgi distribution [20]. We found that this Golgi pool colocalized with coatomer (Fig S2c). We also found that the overexpression of cPLA2–α inhibited retrograde COPI transport in vivo, which was abrogated by a catalytic dead mutation (Fig 2a). Revisiting the reconstitution system, we found that the addition of recombinant cPLA2–α inhibited COPI vesicle formation (Fig 2b). Calcium was needed for the recruitment of recombinant cPLA2–α to Golgi membrane, which could be reversed by BAPTA [1,2-bis(o-aminophenoxy)ethane-N,N,N′,N′-tetraacetic acid], a calcium chelating agent (Fig 2c). Calcium also promoted the ability of cPLA2-α to inhibit vesicle formation, which was again reversed by the addition of BAPTA (Fig 2d).

To examine the role of endogenous cPLA2–α in COPI vesicle formation, we found that the Golgi pool could be reduced by washing Golgi membrane more stringently (Fig S2d). This reduction prevented the ability of MAFP to enhance vesicle formation (Fig S2e). Consistent with this finding, the addition of an antibody against cPLA2–α to the reconstitution system also enhanced vesicle formation (Fig 2e). We also found that the addition of recombinant cPLA2–α to the reconstitution system induced tubule formation (Fig 2f). Thus, we concluded that cPLA2–α opposed the role of LPAAT–γ in modulating vesicle versus tubule formation.

We also sought to confirm more directly that these two enzymatic activities regulated the level of PA on Golgi membrane. PA species were detected on Golgi membrane using mass spectrometry (Figs S3a and S3b). PA level became reduced upon the addition of CI-976 (Figs 3a and S3c) or recombinant cPLA2–α (Fig 3b and S3c). DAG level was also reduced by adding CI-976 (Figs S3d and S3e), which could be attributed to the Golgi possessing a PA phosphatase activity [21]. As control, the levels of multiple other lipids, such as phosphatidylcholine (PC), phosphatidylserine (PS), and sphingomyelin (SM), were unchanged by either perturbation (Figs 3a and 3b).

We next sought to elucidate the mechanistic relationship between the COPI complex and the two lipid enzymatic activities. When an anti-coatomer antibody was added to the reconstitution system, we found that COPI vesicle formation was blocked (Fig 3c). EM analysis revealed that the antibody inhibited the initial stage of bud formation, as Golgi membrane was devoid of protrusive structures (Fig 3d). We also found that the various ways of promoting tubule formation, either by inhibiting LPAAT–γ activity or by promoting cPLA2–α activity, could not overcome the inhibitory effect of the anti-coatomer antibody (Fig 3e). Thus, we concluded that the COPI complex acted initially in promoting bud

formation from Golgi membrane, and then the opposing enzymatic activities of LPAAT–γ and cPLA2–α dictated whether such buds became vesicles or tubules (Fig 3f).

As further support, we next replaced purified protein components in the reconstitution system with cytosol. Tubule formation could also be observed by either inhibiting LPAAT activity using CI-976 or enhancing cPLA2 activity by adding the recombinant protein (Fig S4a). Parallel to these findings, vesicle formation was reduced when LPAAT activity was inhibited or when cPLA2-α activity was promoted (Fig S4b). We also found that the depletion of coatomer reduced the ability of cytosol to support either tubule (Fig S4a) or vesicle (Fig S4b) formation.

We next sought to elucidate physiologic role(s) of COPI tubules. Golgi tubules have been shown recently to be promoted by cPLA2–α activity, and characterized to act in anterograde intra-Golgi transport and Golgi ribbon formation [22]. Thus, we examined whether COPI was also critical for these two events. To avoid a complete disruption of Golgi stacking due to prolonged inhibition of coatomer [23], we pursued the microinjection of an anti-coatomer antibody into cells. This treatment transformed a Golgi marker from a ribbon-like pattern to a dispersed punctate pattern, as assessed by immunofluorescence microscopy (Fig 4a). EM revealed that this transformation represented Golgi ribbons being converted into mini-stacks (Fig 4b and Fig S4c). We also found that the level of Golgi vesicles became reduced (Fig 4c). This effect was not simply a consequence of the Golgi transformation, because the conversion of Golgi ribbons into mini-stacks by a different mechanism (using nocodazole to disrupt microtubules) did not reduce the level of Golgi vesicles significantly (Fig S4d). We next assessed anterograde intra-Golgi transport by tracking the transit of VSVG across the Golgi stacks. Cells microinjected with the anti-coatomer antibody showed delayed arrival of VSVG to the trans-Golgi network (TGN) (Fig 4d). Thus, as the inhibition of coatomer led to similar effects on Golgi ribbon formation and anterograde intra-Golgi transport as previously observed for the inhibition of cPLA2-α, we concluded that Golgi tubules found recently to be promoted by cPLA2-α likely required the COPI complex for their initial generation.

A possibility was that inhibition of anterograde intra-Golgi transport in the microinjected cells was an indirect effect of having inhibited retrograde COPI vesicular transport. To address this issue, we noted that PLD2 had been shown to act in late COPI vesicle fission [14], when the fate of COPI buds should have already been determined in becoming vesicles. We initially confirmed this prediction, as the addition of an antibody against PLD2 did not affect COPI tubule formation (Fig S4e). Subsequently, microinjecting an anti-PLD2 antibody into cells, we found that anterograde intra-Golgi transport of VSVG was also unaffected (Fig 4e). In contrast, this microinjection had been shown previously to inhibit retrograde COPI transport [14]. Thus, we concluded that the anti-coatomer antibody likely exerted a direct inhibition on anterograde intra-Golgi transport.

We also noted that the deletion of either PLD1 [24] or PLD2 [25] in mice had not revealed drastic changes in the early secretory system, which was in contrast to the effects of perturbing coatomer [23]. Thus, we sought to confirm that PLD2 acted in retrograde COPI vesicular transport by another approach, by pursuing acute pharmacologic inhibition. As

assessed by the reconstitution system initially, we found that a PLD2 inhibitor [26], but not a PLD1 inhibitor [27], reduced vesicle formation (Fig S5a). EM confirmed that the late stage of vesicle fission was inhibited (Fig S5b). We also found that only the PLD2, but not the PLD1, inhibitor blocked retrograde COPI transport in vivo by tracking the fate of VSVG-KDELR (Fig S5c). We next found that the PLD2 inhibitor had no significant effect on tubule formation, as assessed by the reconstitution system (Fig S5d). Moreover, the PLD2 inhibitor did not affect anterograde intra-Golgi transport in vivo by tracking the fate of VSVG (Fig S5e). Thus, similar to the effects of antibody microinjection, the use of pharmacologic inhibition also revealed that the acute targeting of PLD2 activity affected only retrograde COPI vesicular transport but not anterograde COPI tubular transport. Notably, this selective role of PLD2 also helped to explain why the deletion of PLD2 did not induce defects in the early secretory system as severe as those seen upon the perturbation of coatomer, as PLD2 only acted in retrograde COPI transport while coatomer acted in bidirectional COPI transport.

We next sought insight into how COPI tubules promoted anterograde intra-Golgi transport. Golgi membrane was collected from cells that expressed either VSVG (as the model anterograde cargo) or VSVG-KDELR (as the model retrograde cargo). Upon the reconstitution of either COPI vesicles or tubules from Golgi membrane, we found that VSVG-KDELR was selectively incorporated into COPI vesicles (Fig 5a). In contrast, both VSVG and VSVG-KDELR were detected in COPI tubules (Fig 5b). To determine why COPI tubules appeared to transport cargoes non-selectively, we pursued EM morphometry, which revealed that both VSVG (Fig 5c) and VSVG-KDELR (Fig 5d) were diffusely distributed along tubular membrane. In contrast, coatomer was concentrated at the tip and base of tubules (Fig 5e). We also scrutinized the electron-dense coating on different membrane structures by EM, and found that COPI buds and vesicles exhibited more obvious coating than COPI tubules (Fig 5f). As confirmation, we assessed the relative density of COPI vesicles versus tubules using density gradients. COPI tubules were released from Golgi membrane by pipette-induced shearing, and as control, reconstituted COPI vesicles were subjected to similar treatment. Whereas COPI vesicles exhibited density equivalent of 43% sucrose, as previously documented [9], COPI tubules exhibited a lighter density (Fig 5g). Thus, when the results were taken altogether, we concluded that cargoes were transported non-selectively in COPI tubules, because the coat complex was not sufficiently concentrated on these membrane structures to allow a more selective mechanism of cargo sorting. Moreover, because anterograde cargoes should have as a concentration gradient at the Golgi complex, which would be higher at the *cis* as compared to the *trans* side (as anterograde cargoes are derived from the ER), the elucidated mechanism of transport for COPI tubules could help drive anterograde transport through the Golgi stacks.

In summary, we have found that the COPI complex is critical for the initial generation of buds from Golgi membrane that can then become either vesicles or tubules. The fate of nascent buds depends on the relative activity of two opposing lipid enzymatic activities. LPAAT–γ promotes the early stage of fission to direct buds in becoming COPI vesicles. In contrast, cPLA2–α, which promotes the converse enzymatic reaction, inhibits early COPI vesicle fission to divert buds in becoming tubules. Moreover, as we have found previously

that PLD2 acts at the late stage of COPI vesicle fission [14], the current finding that LPAAT–γ acts at the early stage of COPI vesicle fission uncovers surprising complexity by which PA acts in the fission process (summarized in Fig 3f). Our current findings also suggest the prospect of resolving an ongoing contentious debate regarding the role of COPI in intra-Golgi transport [28, 29]. Originally, COPI was proposed to form vesicles that act in anterograde transport across the Golgi stacks. In recent years, cisternal maturation has gained favor in explaining anterograde intra-Golgi transport, relegating COPI to act mainly in retrograde transport [28, 29]. Notably, in any of the models that have been considered thus far, COPI has been assumed to act in vesicular transport. In contrast, our finding that COPI also acts in tubular transport, and such carriers promote anterograde transport across the Golgi stacks, now offers a fresh reconciling explanation for how COPI acts in both directions of intra-Golgi transport. We further note that extensive characterization of different coat proteins thus far has only revealed physiologic roles in vesicle formation [1, 2]. Moreover, studies on model systems of tubular transport have not identified coat proteins to play a major role [3, 4]. As such, we have also revealed a mechanistic relationship between vesicular and tubular transport that has been unanticipated.

METHODS

Chemicals, proteins, and cells

The following chemicals were obtained: GTP (Sigma), BEL and MAPF (Cayman Chemical), BAPTA (Invitrogen), CI-976 (GlaxoSmithKline Pharmaceuticals), and bovine serum albumin (Sigma). PA and DAG (C16, C18:1), used as standards for mass spectrometry, were also obtained (Sigma). A PLD1-specific inhibitor, (1R,2R)-N-([S]-1-(4-[5-bromo-2-oxo-2,3-dihydro-1H-benzo(d)imidazol-1-yl]piperidin-1-yl)propan-2-yl)-2-phenylcyclopropanecarboxamide [27], and a PLD2-specific inhibitor, N-(2-[4-oxo-1-phenyl-1,3,8-triazaspiro(4,5)decan-8-yl]ethyl)quinoline-3-carboxamide [26], were obtained from Avanti Polar Lipids. Preparation of coatomer, ARF1, ARFGAP1, BARS, Golgi membrane and cytosol has been described [9, 11]. Preparation of recombinant cPLA2 isoforms has also been described [30]. HeLa cells were cultured as previously described [11].

Plasmids and antibodies

VSVG and VSVG-KDELR in mammalian expression vectors have been described previously [11, 18]. Both contain a temperature-sensitive mutation of VSVG (ts-045). Human LPAAT-γ cDNA was inserted into *EcoR1* and *EcoRV* sites of the mammalian expression vector p3xFlag-CMV. A catalytic dead mutant (H96A) [31] was generated using the QuikChange Site-Directed-Mutagenesis Kit (Stratagene) and the paired oligonucleotides: 5′-GCAGTCATCATCCTCAACGCCAACTTCGAGATCGACTTCC-3′ and 5′-GGAAGTCGATCTCGAAGTTGGCGTTGAGGATGATGACTGC-3′. Human cPLA2–α and the corresponding catalytic-dead point mutant were inserted into *HindIII* and *PstI* sites of the mammalian expression vector pECFP(C3).

Mouse antibodies have been described, including: anti-β–COP (M3A5 culture supernatant used at 1:3 dilution), anti-VSVG (BW8G65 culture supernatant, 1:10 dilution), anti-Myc (9E10 culture supernatant, 1:10 dilution) and anti-coatomer (CM1A10 culture supernatant,

1:10 dilution) antibodies [9, 11, 18, 32]. Rabbit antibodies have also been described [9, 11, 14, 18, 22], including: anti-cPLA2-α (used at 1:500 dilution), anti-mannosidase I (1:500 dilution), anti-εCOP (1:500 dilution), anti-ζ-COP (1:500 dilution), anti-KDELR (1:500), and anti-PLD2 (1:1000 dilution). An antibody against human LPAAT-γ was generated by injecting rabbits with the central domain (residues 78–300) as a recombinant protein, and used at 1:1000 dilution. A rabbit anti-α–COP antibody (1:500 dilution) was obtained (kind gift by F. Wieland, Heidelberg, Germany). Secondary antibodies that were obtained (Jackson ImmunoResearch) include: Cy2-or Cy3-conjugated donkey antibodies against mouse or rabbit IgG (both used at 1:200 dilution), horseradish peroxidase-conjugated donkey antibodies against mouse or rabbit IgG (both used at 1:20,000 dilution). 10-nm gold-conjugated goat antibodies against rabbit IgG (used at 1:250 dilution) was also obtained (Sigma).

In vitro reconstitution system

The COPI reconstitution system was performed as previously described [11]. Briefly, Golgi membrane (0.2 mg/ml) was washed with 3M KCl, and then incubated with ARF1 (6 μg/ml) and coatomer (6 μg/ml) for the first-stage incubation that reproduces the ARF-dependent recruitment of coatomer onto Golgi membrane. The Golgi membrane was re-isolated and then incubated with ARFGAP1 (2 μg/ml) and BARS (2 μg/ml) for the second stage that results in vesicle formation. Although PLD2 is also required for COPI vesicle formation [14], it was not added to the reconstitution system, because an endogenous pool remained on Golgi membrane after washing with 3M KCl [14]. CI-976 was used at 20 μM. PLD inhibitors were used at 1 μM. For the initial characterization of PLA2 activity on Golgi membrane that involved pharmacologic inhibition, the membrane was washed with 0.5M KCl to allow endogenous PLA2 activity to remain on Golgi membrane. Doses of BEL and MAFP used in these studies are indicated in individual figures. Reconstitutions that added the recombinant forms of cPLA2 (0.6 μg/ml) used Golgi membrane washed with 3M KCl. For antibody blocking studies, Golgi membranes (100μg) was also washed with 0.5M KCl to retain an endogenous pool of the targeted protein, followed by antibody addition (5 μl).

To examine cargoes in COPI tubules versus vesicles, COS-1 cells were transiently transfected with either VSVG or VSVG-KDELR, followed by isolation of Golgi membrane from these cells. Cells that express VSVG-KDELR were incubated at the permissive temperature (32°C), as this chimera resides mostly at the Golgi at this temperature. In contrast, cells that express VSVG were shifted from the non-permissive temperature (39°C) to the permissive temperature (32°C) for 10 minutes to collect a synchronized pool of this chimera at the Golgi.

Electron microcopy

Examination of Golgi membrane or reconstituted vesicles using the whole-mount technique has been described previously [9, 11]. Examination of cells after epon-embedding followed by serial thin sectioning has also been described previously [33]. Quantitation was performed as described in figure legends.

Transfections and siRNA and rescue

Transfection of DNA plasmids was performed using FuGene6 (Roche). Transfection of siRNA was performed using Oligofectamine (Invitrogen). The siRNA sequence used to target human LPAAT-γ (GAGACCAAGCACCGCGTTA) was obtained (Dharmacon). Rescue plasmids for wild-type and catalytic dead mutant of human LPAAT-γ were generated by targeting this siRNA sequence using the QuikChange Site-Directed-Mutagenesis Kit (Stratagene) with paired oligonucleotides: 5′-CGCTTCACGGAGACCAAGCATAGGGTTAGCATGGAGGTGGCG-3′ and 5′-CGCCACCTCCATGCTAACCCTATGCTTGGTCTCCGTGAAGCG-3′.

In vivo transport assays

COPI retrograde transport as assessed by the redistribution of VSVG-KDELR has been described previously [11, 18]. Anterograde transport of VSVG has also been described previously [22, 34]. PLD inhibitors were added at 100 nM.

Microinjections

Microinjection of antibodies (1 mg/ml) was performed as previously described [34].

Lipid analysis

Golgi lipids were measured using comparative mass spectrometry [35]. Briefly, Golgi membrane in assay buffer [25mM Hepes pH7.2, 50mM KCl, 2.5mM $Mg(OAc)_2$, and 200mM sucrose] was extracted [36] with 4ml of $CHCl_3/CH_3OH$ (2/1, v/v) and 2ml of PBS-saturated $CHCl_3/CH_3OH$ (2/1, v/v) successively. Organic phases were pooled and dried under vacuum (GeneVac). The remaining aqueous phase was acidified with cold acetic acid to pH 3–4 and extracted two times with 2ml of cold PBS-saturated $CHCl_3/CH_3OH$ (2/1, v/v). Organic phases were pooled and neutralized with cold 10% trietylamine in $CHCl_3/CH_3OH$ (2/1, v/v). The neutralized organic phase was combined to initial extractions and dried under vacuum. Lipid detection was performed using liquid chromatography coupled to tandem mass spectrometry (LC-MS/MS) in negative mode (Agilent 6520 Q-TOF mass spectrometer combined to an Agilent 1200 series HPLC system), essentially as previously described [35]. Briefly, chromatography was performed using a silica column (5μ, 100 × 2.1mm). Solvent A was hexanes/isopropanol 50/50 (v/v), 0.02% NH4OH, 0.01% HCOOH and B solvent hexanes/isopropanol/water 30/60/15 (v/v/v) 0.02% NH_4OH, 0.01% HCOOH. Solvents gradient was (0.15ml/min): 0–8 min; 100% A, 8–13 min; 0–100% linear B, 13–18 min; 100% B and 18–23min; 0–100% linear A, followed by a 10 min conditioning post-run (100% A). 20 ul of the dried Golgi membrane lipid extract resuspended in 50μl of solvent A was injected per analysis. The different PA forms were detected in the Golgi lipidic extract at the same retention time (5.5 min) as a standard (C16, C18:1) with a mass accuracy of 1–5 ppm. The different DAG forms were detected at the same retention time (1.1 to 1.3 min) as a standard (C16, C18:1) with a mass accuracy of < 1ppm. The PA molecular species assignment was confirmed by collisional experiments performed in negative mode using a 25V collision energy. Other lipid species were assigned based on previously described polarity and on the accuracy of the detected m/z (1.2 ppm).

Statistical analysis

Student's t-test was used to analyze statistical significance.

Supplementary Material

Refer to Web version on PubMed Central for supplementary material.

Acknowledgments

We thank Jian Li and Ming Bai for advice and discussions, Giuseppe Di Tullio and Michele Santoro for generating the anti-LPAAT-γ antibody, and Robyn Loper for technical assistance. This work is funded by grants from the National Institutes of Health to VWH (GM058615), DBM (AI071155 and AR048632), CCL (HL061378), MHG (HL050040), WJB (GM051596), and also by grants from Telethon to AL (GGPO823) and RP (GTF08001), from AIRC to AL (IG4700), DC (IG4664) and RP (IG10233), and from European Grant Eucilia to AL (HEALT-F2-2007-201804). CV is a recipient of an Italian Foundation for Cancer Research Fellowship. DBM is supported by the Burroughs Wellcome Fund Program in Translational Medicine.

References

1. Cai H, Reinisch K, Ferro-Novick S. Coats, tethers, Rabs, and SNAREs work together to mediate the intracellular destination of a transport vesicle. Dev Cell. 2007; 12:671–682. [PubMed: 17488620]
2. Pucadyil TJ, Schmid SL. Conserved functions of membrane active GTPases in coated vesicle formation. Science. 2009; 325:1217–1220. [PubMed: 19729648]
3. Bard F, Malhotra V. The formation of TGN-to-plasma-membrane transport carriers. Annu Rev Cell Dev Biol. 2006; 22:439–455. [PubMed: 16824007]
4. De Matteis MA, Luini A. Exiting the Golgi complex. Nat Rev Mol Cell Biol. 2008; 9:273–284. [PubMed: 18354421]
5. Hsu VW, Lee SY, Yang JS. The evolving understanding of COPI vesicle formation. Nat Rev Mol Cell Biol. 2009; 10:360–364. [PubMed: 19293819]
6. Waters MG, Serafini T, Rothman JE. 'Coatomer': a cytosolic protein complex containing subunits of non-clathrin-coated Golgi transport vesicles. Nature. 1991; 349:248–251. [PubMed: 1898986]
7. Donaldson JG, Cassel D, Kahn RA, Klausner RD. ADP-ribosylation factor, a small GTP-binding protein, is required for binding of the coatomer protein beta-COP to Golgi membranes. Proc Natl Acad Sci USA. 1992; 89:6408–6412. [PubMed: 1631136]
8. Cukierman E, Huber I, Rotman M, Cassel D. The ARF1-GTPase-Activating Protein: Zinc finger motif and Golgi complex localization. Science. 1995; 270:1999–2002. [PubMed: 8533093]
9. Yang JS, et al. ARFGAP1 promotes the formation of COPI vesicles, suggesting function as a component of the coat. J Cell Biol. 2002; 159:69–78. [PubMed: 12379802]
10. Lee SY, Yang JS, Hong W, Premont RT, Hsu VW. ARFGAP1 plays a central role in coupling COPI cargo sorting with vesicle formation. J Cell Biol. 2005; 168:281–290. [PubMed: 15657398]
11. Yang JS, et al. A role for BARS at the fission step of COPI vesicle formation from Golgi membrane. EMBO J. 2005; 24:4133–4143. [PubMed: 16292346]
12. Weigert R, et al. CtBP/BARS induces fission of Golgi membranes by acylating lysophosphatidic acid. Nature. 1999; 402:429–433. [PubMed: 10586885]
13. Gallop JL, Butler PJ, McMahon HT. Endophilin and CtBP/BARS are not acyl transferases in endocytosis or Golgi fission. Nature. 2005; 438:675–678. [PubMed: 16319893]
14. Yang JS, et al. A role for phosphatidic acid in COPI vesicle fission yields insights into Golgi maintenance. Nat Cell Biol. 2008; 10:1146–1153. [PubMed: 18776900]
15. Chambers K, Judson B, Brown WJ. A unique lysophospholipid acyltransferase (LPAT) antagonist, CI-976, affects secretory and endocytic membrane trafficking pathways. J Cell Sci. 2005; 118:3061–3071. [PubMed: 15972316]
16. Shindou H, Shimizu T. Acyl-CoA:lysophospholipid acyltransferases. J Biol Chem. 2009; 284:1–5. [PubMed: 18718904]

17. Schmidt JA, Brown WJ. Lysophosphatidic acid acyltransferase 3 regulates Golgi complex structure and function. J Cell Biol. 2009; 186:211–218. [PubMed: 19635840]
18. Yang JS, et al. Key components of the fission machinery are interchangeable. Nat Cell Biol. 2006; 8:1376–1382. [PubMed: 17086176]
19. Schaloske RH, Dennis EA. The phospholipase A2 superfamily and its group numbering system. Biochim Biophys Acta. 2006; 1761:1246–1259. [PubMed: 16973413]
20. Evans JH, Spencer DM, Zweifach A, Leslie CC. Intracellular calcium signals regulating cytosolic phospholipase A2 translocation to internal membranes. J Biol Chem. 2001; 276:30150–30160. [PubMed: 11375391]
21. Asp L, et al. Early stages of Golgi vesicle and tubule formation require diacylglycerol. Mol Biol Cell. 2009; 20:780–790. [PubMed: 19037109]
22. San Pietro E, et al. Group IV phospholipase A(2)alpha controls the formation of inter-cisternal continuities involved in intra-golgi transport. PLoS Biol. 2009; 7:e1000194. [PubMed: 19753100]
23. Guo Q, Vasile E, Krieger M. Disruptions in Golgi structure and membrane traffic in a conditional lethal mammalian cell mutant are corrected by epsilon-COP. J Cell Biol. 1994; 125:1213–1224. [PubMed: 8207054]
24. Dall'Armi C, et al. The phospholipase D1 pathway modulates macroautophagy. Nature communications. 2010; 1:142.
25. Oliveira TG, et al. Phospholipase d2 ablation ameliorates Alzheimer's disease-linked synaptic dysfunction and cognitive deficits. J Neurosci. 2010; 30:16419–16428. [PubMed: 21147981]
26. Lavieri R, et al. Design and synthesis of isoform-selective phospholipase D (PLD) inhibitors. Part II. Identification of the 1,3,8-triazaspiro[4,5]decan-4-one privileged structure that engenders PLD2 selectivity. Bioorganic & medicinal chemistry letters. 2009; 19:2240–2243. [PubMed: 19299128]
27. Lewis JA, et al. Design and synthesis of isoform-selective phospholipase D (PLD) inhibitors. Part I: Impact of alternative halogenated privileged structures for PLD1 specificity. Bioorganic & medicinal chemistry letters. 2009; 19:1916–1920. [PubMed: 19268584]
28. Emr S, et al. Journeys through the Golgi--taking stock in a new era. J Cell Biol. 2009; 187:449–453. [PubMed: 19948493]
29. Glick BS, Nakano A. Membrane traffic within the Golgi apparatus. Annu Rev Cell Dev Biol. 2009; 25:113–132. [PubMed: 19575639]
30. de Carvalho MG, et al. Identification of phosphorylation sites of human 85-kDa cytosolic phospholipase A2 expressed in insect cells and present in human monocytes. J Biol Chem. 1996; 271:6987–6997. [PubMed: 8636128]
31. Yuki K, Shindou H, Hishikawa D, Shimizu T. Characterization of mouse lysophosphatidic acid acyltransferase 3: an enzyme with dual functions in the testis. Journal of lipid research. 2009; 50:860–869. [PubMed: 19114731]
32. Palmer DJ, Helms JB, Beckers CJ, Orci L, Rothman JE. Binding of coatomer to Golgi membranes requires ADP-ribosylation factor. J Biol Chem. 1993; 268:12083–12089. [PubMed: 8505331]
33. Kweon HS, et al. Golgi enzymes are enriched in perforated zones of golgi cisternae but are depleted in COPI vesicles. Mol Biol Cell. 2004; 15:4710–4724. [PubMed: 15282336]
34. Bonazzi M, et al. CtBP3/BARS drives membrane fission in dynamin-independent transport pathways. Nat Cell Biol. 2005; 7:570–580. [PubMed: 15880102]
35. Siegrist MS, et al. Mycobacterial Esx-3 is required for mycobactin-mediated iron acquisition. Proc Natl Acad Sci U S A. 2009; 106:18792–18797. [PubMed: 19846780]
36. Bollinger JG, Ii H, Sadilek M, Gelb MH. Improved method for the quantification of lysophospholipids including enol ether species by liquid chromatography-tandem mass spectrometry. Journal of lipid research. 51:440–447. [PubMed: 19717841]

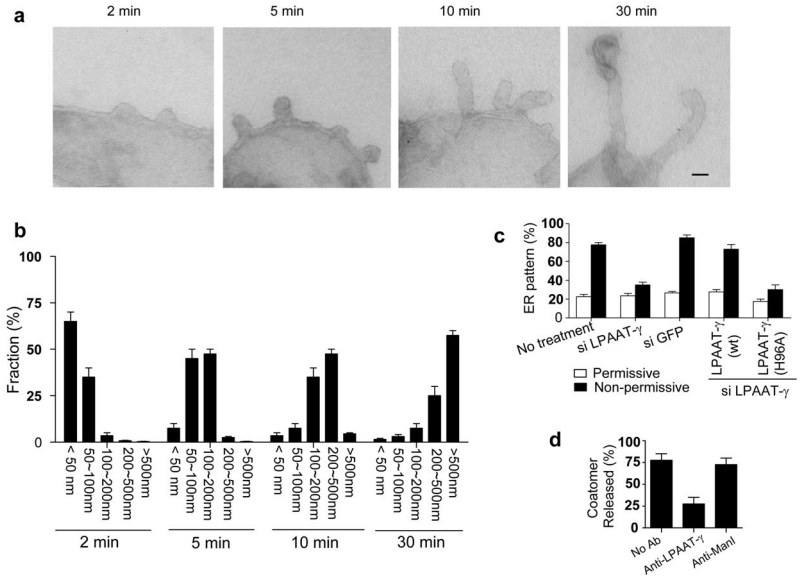

Figure 1. LPAAT activity promotes COPI vesicle formation and inhibits tubule formation from Golgi membrane

(a) Examination of Golgi membrane by EM upon incubation with CI-976 in the COPI reconstitution system; bar, 50 nm.

(b) Quantitation of Golgi tubules seen upon the addition of CI-976 to the reconstitution system. Golgi tubules within particular lengths, as indicated, were quantified, and then grouped and expressed as a fraction of total. The mean from three experiments with standard error is shown.

(c) COPI-dependent retrograde transport, as tracked by the redistribution of VSVG-KDELR from the Golgi to the ER, requires the catalytic activity of LPAAT–γ. HeLa cells were treated with siRNA against LPAAT–γ or against an irrelevant sequence (encoded by GFP), and also transfected with VSVG-KDELR. For rescues, cells were also transfected with a siRNA-resistant form of wild-type (wt) or catalytic-dead point mutant (H96A). The ER pattern for the chimeric KDELR was then quantified. The mean from three experiments with standard error is shown.

(d) An anti-LPAAT-γ antibody inhibits COPI vesicle formation. Antibodies as indicated were incubated with Golgi membrane, and then added to the COPI reconstitution system. The release of β-COP from Golgi membranes after the second-stage incubation was then quantified. The mean from three experiments with standard error is shown.

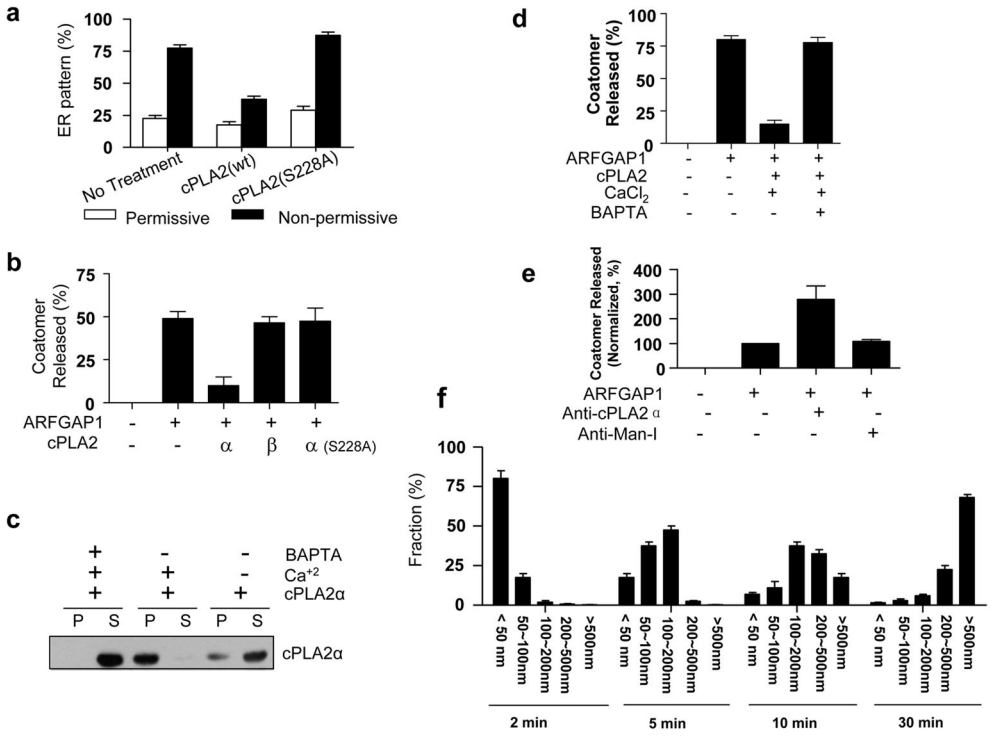

Figure 2. PLA2 activity inhibits COPI vesicle formation and promotes tubule formation

(a) Inhibition of retrograde COPI transport requires the catalytic activity of cPLA2–α. HeLa cells were transfected with wild-type (wt) or catalytic-dead point mutant (S228A) of cPLA2–α, and then quantified for an ER pattern of VSVG-KDELR. The mean from three experiments with standard error is shown.

(b) Inhibition of COPI vesicle formation by cPLA2-α. The reconstitution system was performed, with the second-stage incubation containing components as indicated. BARS was added in all conditions. After centrifugation, β–COP in the pellet and supernatant fractions were quantified, and then calculated for the fractional release. The mean from three experiments with standard error is shown.

(c) Binding of recombinant cPLA2–α to Golgi membrane requires calcium. After incubation of the recombinant protein with Golgi membrane in conditions as indicated, centrifugation was performed to pellet Golgi membrane followed by immunoblotting for cPLA2–α. Full scan of the gel is shown as Supplementary information.

(d) Inhibition of COPI vesicle formation by cPLA2–α requires calcium. The reconstitution system was performed, with the second-stage incubation containing components as indicated. BARS was added in all conditions. The mean from three experiments with standard error is shown.

(e) An anti-cPLA2–α antibody added to Golgi membrane promotes COPI vesicle formation. The reconstitution system was performed using Golgi membrane washed with 0.5M KCl. ARFGAP1 was added at reduced level, so that potential enhancement in COPI vesicle formation above the basal level could be more readily detected. The fractional release of β–COP from Golgi membrane after the second-stage incubation was normalized to control (no antibody added). The mean from three experiments with standard error is shown.

(f) Quantitation of Golgi tubules seen upon adding recombinant cPLA2–α to the reconstitution system. The reconstitution system was performed, with the second-stage incubation containing ARFGAP1, BARS, and recombinant cPLA2–α. Subsequently, Golgi tubules within particular lengths, as indicated, were quantified, and then grouped and expressed as a fraction of total. The mean from three experiments with standard error is shown.

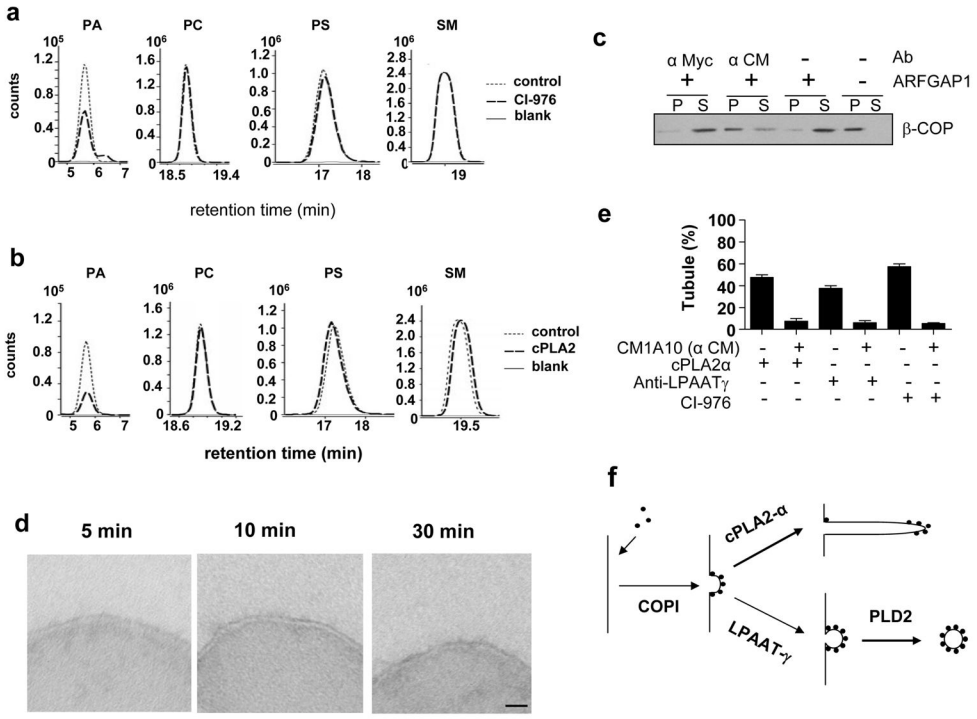

Figure 3. The relative roles of COPI and lipid enzymes in vesicle versus tubule formation

(a) Adding CI-976 reduces PA on Golgi membrane. Golgi membrane was incubated with or without CI-976, followed by lipid extraction and comparative LC-MS analysis. Blank indicates injection with solvent.

(b) Adding cPLA2–α reduces PA on Golgi membrane. Golgi membrane was incubated with or without recombinant cPLA2–α, followed by lipid extraction and comparative LC-MS analysis. Blank indicates injection with solvent.

(c) The anti-coatomer antibody inhibits COPI vesicle formation. The reconstitution system was performed with the anti-coatomer antibody (CM1A10) also added to the incubation. Vesicle formation was assessed by the release of β–COP from Golgi membrane after the second-stage incubation. Full scan of the gel is shown as Supplementary information.

(d) Bud formation from Golgi membrane is inhibited by an anti-coatomer antibody. The antibody was added to the reconstitution system followed by examination of Golgi membrane using EM. Representative images are shown; bar, 50 nm.

(e) Tubule formation is inhibited by the anti-coatomer antibody. The reconstitution system was performed with additional components as indicated. The level of tubules (> 100 nm in length) was then quantified by EM, and expressed as a percentage of all protrusions seen on Golgi membrane. The mean from three experiments with standard error is shown.

(f) Summarizing how key determinants act in COPI vesicle versus tubule formation. The COPI complex initially drives the formation of buds from Golgi membrane. Subsequently, cPLA2–α activity promotes elongation of these buds to become tubules. In contrast, LPAAT–γ activity commits these buds toward vesicle formation by promoting the early stage of fission, which initiates the constriction of the bud neck, followed by PLD2 activity that completes vesicle fission.

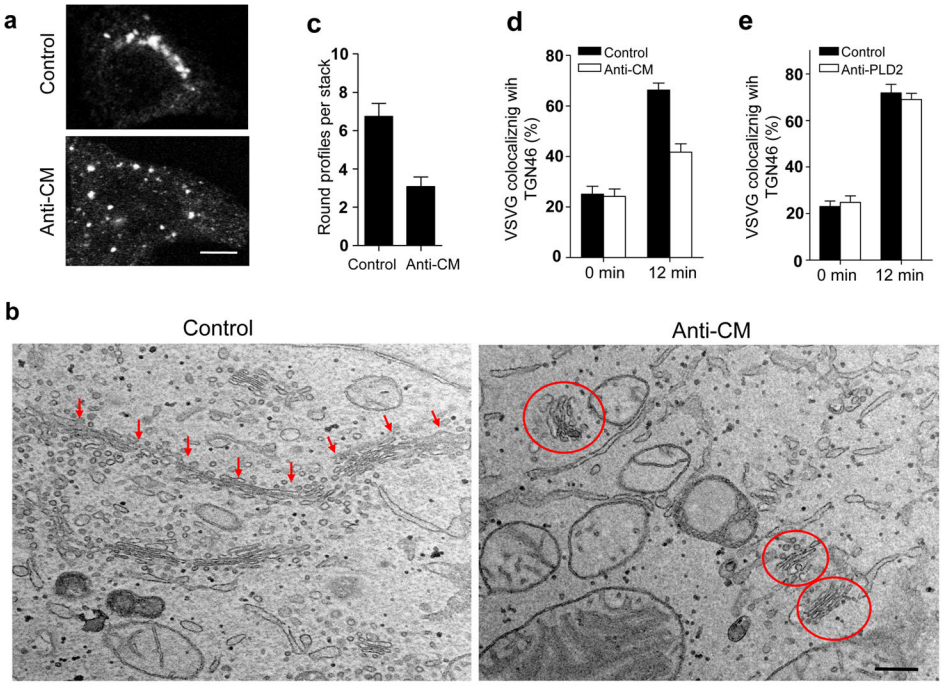

Figure 4. Characterizing how COPI acts in Golgi structure and transport

(a) Microinjection of an anti-coatomer antibody transforms the Golgi from ribbons to dispersed punctate structures. HeLa cells were microinjected with the anti-coatomer antibody or with vehicle as control, followed by examination using immunofluorescence microscopy to assess the distribution of a Golgi marker (TGN46); bar, 5 um.

(b) Microinjection of the anti-coatomer antibody transforms Golgi ribbons to mini-stacks. EM was then performed after microinjection; bar, 400 nm. In control cells, the Golgi exhibits an extended ribbon structure, which is highlighted by the row of red arrows. In cells with coatomer inhibited, the Golgi is converted into “mini-stacks,” which is highlighted by red circles.

(c) Microinjection of the anti-coatomer antibody reduces the level of Golgi vesicles. HeLa cells were microinjected with the anti-coatomer antibody or with vehicle as control. The level of Golgi-associated vesicles was then quantified. The mean from three experiments with standard error is shown.

(d) Anterograde transport through the Golgi stacks is inhibited by the anti-coatomer antibody. VSVG-ts045 was expressed in HeLa cells, and then allowed to accumulate at the pre-Golgi compartment by shifting cell incubation from 40°C to 15°C. Cells were then microinjected with the anti-coatomer antibody or with vehicle, and then shifted to 20°C for times indicated. Colocalization of VSVG-ts045 with TGN46 was subsequently quantified. The mean from three experiments with standard error is shown.

(e) Anterograde transport through the Golgi stacks is not affected by an anti-PLD2 antibody. A similar experiment was performed as described above, except HeLa cells were microinjected with an anti-PLD2 antibody. The mean from three experiments with standard error is shown.

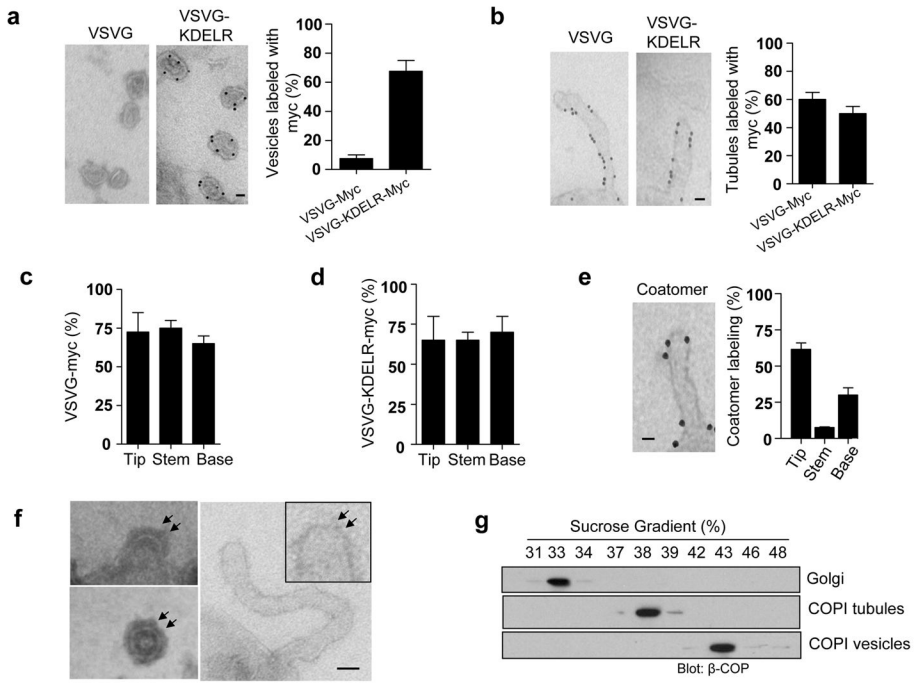

Figure 5. Characterizing cargo transport in COPI tubules

(a) COPI vesicles contain retrograde but not anterograde cargo.

COPI vesicles were reconstituted from Golgi membrane that expressed either VSVG-myc or VSVG-KDELR-myc, followed by immunogold labeling for the myc tag. Representative EM images are shown (left); bar, 25 nm. Quantitation was also performed (right), with the mean and standard error from three experiments shown.

(b) COPI tubules contain both anterograde and retrograde cargoes.

The same experiment as described above was performed, except COPI tubules were reconstituted by adding cPLA2–α at the second stage. Representative EM images are shown (left); bar, 25 nm. Quantitation was also performed (right), with the mean and standard error from three experiments shown.

(c) VSVG is diffusely distributed along COPI tubules.

The distribution of VSVG at the tip, base, and stem of 30 tubules was quantified, and then expressed as a fraction of total. The mean with standard error from three experiments is shown.

(d) VSVG-KDELR is diffusely distributed along COPI tubules.

A similar analysis as described above was performed to track VSVG-KDELR. The mean from three experiments with standard error is shown.

(e) Coatomer is concentrated at the tip and base of COPI tubules.

Immunogold EM using the anti-α– COP antibody was performed on reconstituted COPI tubules, with a representative EM image shown (left); bar, 25 nm. The distribution of coatomer along three segments of tubular membrane (within 100 nm of the tip, within 100 nm of the base, and in-between) was quantified for 30 tubules, and then expressed as a fraction of the total. The mean with standard error from three experiments is shown.

(f) Comparison of electron-dense coating on COPI buds, vesicles, and tubules. Representative high-resolution EM images of all three membrane structures are shown; bar, 50 nm. Arrows highlight the thickness of coating on membrane structures.
(g) Comparison of membrane density. COPI vesicles, tubules, or Golgi membrane was subjected to equilibrium centrifugation followed by immunoblotting for β–COP. Full scan of the gel is shown as Supplementary information.